Evidence for a Competition between the Superconducting State and the Pseudogap State of $(BiPb)_2(SrLa)_2CuO_{6+\delta}$ from Muon Spin Rotation Experiments

R. Khasanov,[1,2,*] Takeshi Kondo,[3,4] S. Strässle,[2] D. O. G. Heron,[5] A. Kaminski,[3] H. Keller,[2] S. L. Lee,[5] and Tsunehiro Takeuchi[4,6]

[1]*Laboratory for Muon Spin Spectroscopy, Paul Scherrer Institut, CH-5232 Villigen PSI, Switzerland*
[2]*Physik-Institut der Universität Zürich, Winterthurerstrasse 190, CH-8057 Zürich, Switzerland*
[3]*Ames Laboratory and Department of Physics and Astronomy, Iowa State University, Ames, Iowa 50011, USA*
[4]*Department of Crystalline Materials Science, Nagoya University, Nagoya 464-8603, Japan*
[5]*School of Physics and Astronomy, University of St. Andrews, Fife, KY16 9SS, United Kingdom*
[6]*EcoTopia Science Institute, Nagoya University, Nagoya 464-8603, Japan*

(Received 11 June 2008; published 24 November 2008)

The in-plane magnetic penetration depth λ_{ab} in optimally doped $(BiPb)_2(SrLa)_2CuO_{6+\delta}$ (OP Bi2201) was studied by means of muon-spin rotation. The measurements of $\lambda_{ab}^{-2}(T)$ are inconsistent with a simple model of a *d*-wave order parameter and a uniform quasiparticle weight around the Fermi surface. The data are well described assuming the angular gap symmetry obtained in ARPES experiments [Phys. Rev. Lett. **98**, 267004 (2007)], which suggest that the superconducting gap in OP Bi2201 exists only in segments of the Fermi surface near the nodes. The remaining parts of the Fermi surface, which are strongly affected by the pseudogap state, do not contribute significantly to the superconducting condensate.

DOI: 10.1103/PhysRevLett.101.227002 PACS numbers: 74.72.Hs, 74.25.Jb, 76.75.+i

The relevance of the pseudogap phenomenon for superconductivity is an important open issue in the physics of high-temperature cuprate superconductors (HTS's). There are two main scenarios to be considered. In the first, the so-called ''precursor scenario'', the Cooper pairs are already formed at T^*, the temperature at which the pseudogap opens first, but long-range phase coherence is not established until the sample is cooled below the superconducting transition temperature T_c. In the second, the so-called ''two-gap'' scenario, the superconducting and the pseudogap state are not directly related with each other, and may even compete. Within this scenario the gaps in *k*-space, existing near the nodes and in the antinodal region of the Fermi surface, are due to the superconducting and the pseudogap states, respectively. This scenario gained support due to a number of recent experiments [1–5] which revealed that the antinodal gap remains unaffected as the temperature changes across T_c, and generally its magnitude increases significantly in the underdoped region, where T_c decreases. In contrast, the gap near the nodes scales with T_c and obeys a well-defined BCS temperature dependence [4]. This interpretation also agrees with recent results from scanning-tunneling-microscopy experiments [6], suggesting that the incoherent antinodal states are not responsible for the formation of phase-coherent Cooper pairs. Consequently, superconductivity is caused by the coherent part of the Fermi surface near the nodes.

Measurements of the magnetic penetration depth λ can be used to distinguish between the above described scenarios. The temperature dependence of λ is uniquely determined by the absolute maximum value of the superconducting energy gap and its angular and temperature dependence. In addition, within the London model, λ^{-2} is proportional to the superfluid density via $\lambda^{-2} \propto \rho_s \propto n_s/m^*$ and, in case where the supercarrier mass m^* is known, gives information on the supercarrier density n_s.

Here we report on a study of the in-plane magnetic penetration depth λ_{ab} in optimally doped $(BiPb)_2 \times (SrLa)_2CuO_{6+\delta}$ (OP Bi2201). This superconductor was chosen for the following reasons: (i) The angular dependence of the energy gap in similar OP Bi2201 samples was recently studied by Kondo *et al.* [3] by means of angular-resolved photoemission (ARPES); (ii) the maximum values of two spectral gaps, dominating different regions of the Fermi surface, are differ for more than a factor 3. Note that in OP Bi2212 those gaps were found to be almost the same [4]. Good agreement with the ARPES data was obtained within a model which assumes that the pseudogap affects the spectral density of the antinodal quasiparticle. Consequently, only carriers close to the nodes contribute to the superfluid density, while the weight of the coherent quasiparticle near the antinodes is negligible. This statement is also supported by comparing the zero-temperature value of $\lambda_{ab}^{-2}(0)$ for OP Bi2201 studied here with those of other OP HTS's, such as $Ca_{2-x}Na_xCuO_2Cl_2$ (OP Na-CCOC) [7] and $La_{2-x}Sr_xCuO_4$ (OP La214) [8], having similar transition temperatures. It was observed that in superconductors where the superconducting gap is developed only close to the nodes (OP Bi2201 and OP Na-CCOC) the superfluid density is more than 50% smaller than in OP La214 where the *d*-wave superconducting gap is detected on the whole Fermi surface [9].

Details on the sample preparation for OP Bi2201 single crystals can be found elsewhere [10]. The values of T_c and the width of the superconducting transition, as determined from magnetization measurements, are $\simeq$35 K and $\simeq$3 K,

respectively. The transverse-field μSR experiments were carried out at the πM3 beam line at the Paul Scherrer Institute (Villigen, Switzerland). The description of TF-μSR technique and its application to study HTS's can be found in Ref. [11]. Two OP Bi2201 single crystals with an approximate size of $4 \times 2 \times 0.1$ mm^3 were used. The sample was field cooled from above T_c to 1.6 K in a series of fields ranging from 5 to 640 mT. The magnetic field was applied parallel to the crystallographic c axis and transverse to the muon-spin polarization. The typical counting statistics were ~15–18 million muon detections per data point. In order to describe the asymmetric local magnetic field distribution $P(B)$ in the superconductor in the mixed state the analysis of the data was based on a two-component Gaussian fit of the μSR time spectra [12,13]:

$$P(t) = \sum_{i=1}^{2} A_i \exp(-\sigma_i^2 t^2/2) \cos(\gamma_\mu B_i t + \phi), \qquad (1)$$

which corresponds to the field distribution:

$$P(B) = \gamma_\mu \sum_{i=1}^{2} \frac{A_i}{\sigma_i} \exp\left(-\frac{\gamma_\mu^2 (B - B_i)^2}{2\sigma_i^2}\right). \qquad (2)$$

Here A_i, σ_i, and B_i are the asymmetry, the relaxation rate, and the mean field of the ith component, $\gamma_\mu = 2\pi \times 135.5342$ MHz/T denotes the muon gyromagnetic ratio, and ϕ is the initial phase of the muon-spin ensemble. The analysis was simplified to a single Gaussian line shape in the case when the two-Gaussian and the one-Gaussian fits result in comparable χ^2.

The magnetic field penetration depth λ was derived from the total second moment of $P(B)$:

$$\sigma_{\rm tot}^2 = \sum_{i=1}^{2} \frac{A_i}{A_1 + A_2} [\sigma_i^2 + \gamma_\mu^2 [B_i - \langle B \rangle]^2], \qquad (3)$$

as $\lambda^{-4} \propto \sigma_{\rm tot}^2 - \sigma_{\rm nm}^2 = \sigma_{\rm sc}^2$. Here $\sigma_{\rm nm}$ is the nuclear moment contribution, $\sigma_{\rm sc}$ is the superconducting state contribution, and $\langle B \rangle$ is the first moment of $P(B)$ (see Ref. [12] for details). Since the magnetic field was applied along the crystallographic c axis, our experiments provide direct information on λ_{ab}.

Figure 1(a) shows the dependence of $\sigma_{\rm sc}$ on the applied magnetic field measured after field cooling the OP Bi2201 sample from $T > T_c$ down to 1.6 K. The $P(B)$ distributions were calculated using the maximum entropy Fourier-transform technique for $\mu_0 H = 5$, 40, and 640 mT [see Fig. 1(a)]. In the whole range of fields (5 mT $\leq \mu_0 H \leq$ 640 mT) $P(B)$ is asymmetric. The asymmetric shape of $P(B)$ is generally described by the skewness parameter $\alpha_s = \langle \Delta B^3 \rangle^{1/3} / \langle \Delta B^2 \rangle^{1/2}$ [$\langle \Delta B^n \rangle$ is the nth central moment of $P(B)$]. The variation of α_s reflects underlying changes in the vortex structure [14]. In the limit $\kappa \gg 1$ and for realistic measuring conditions $\alpha_s \simeq 1.2$ for an ideal triangular vortex lattice (VL). It is very sensitive to structural changes of the VL which can occur as a function of temperature and/or magnetic field [14,15]. Figure 1(b) implies that in

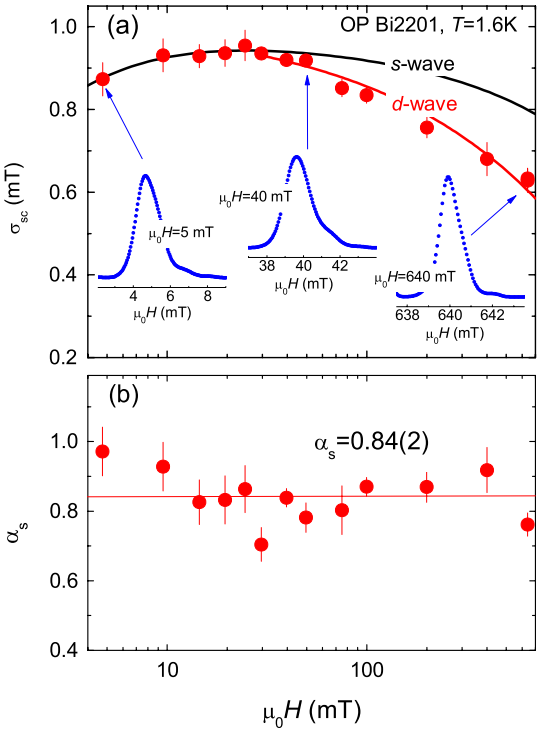

FIG. 1 (color online). (a) Dependence of $\sigma_{\rm sc}$ of OP Bi2201 on the applied magnetic field measured at $T = 1.6$ K. The black solid line corresponds to $\sigma_{\rm sc}(H)$ obtained by using the numerical calculations of Brandt [20] ($\lambda = 360$ nm, $\kappa = 140$) for a superconductor with an isotropic energy gap. The solid red line represents $\sigma_{\rm sc}(H)$ expected in case of a d-wave superconductor. The blue dotted curves show the local magnetic field distribution $P(B)$ calculated by means of the maximum entropy Fourier-transform technique at $T = 1.6$ K and $\mu_0 H = 5$, 40, and 640 mT. (b) Field dependence of the skewness parameter α_s. The solid line is the average value $\alpha_s = 0.84(2)$.

OP Bi2201 $\alpha_s(H)$ is almost constant [$\alpha_s = 0.84(2)$] and is smaller than the expected value of 1.2, which can be caused by microscopic field gradients due to interaction of flux expulsion with pinning, different geometric factors due to the range of crystal sizes and shapes, spatial variation in the penetration depth [16].

It should be noted here that addition of Pb does not change T_c and the in-plane superfluid density $\rho_s \propto \lambda_{ab}^{-2}$ [17], but makes OP Bi2201 *more* three dimensional. To estimate the anisotropy coefficient $\gamma_{c,ab} = \lambda_c / \lambda_{ab}$ (λ_c is the c-axis component of the penetration depth) we performed torque magnetization experiment on one of the crystals studied [18]. A value of $\gamma_{c,ab} \simeq 20$ was found, which is more than 10 times smaller than $\gamma_{c,ab} \simeq 200 - 400$ obtained on OP Bi2201 without Pb by Kawamata *et al.* [19].

Figure 1 indicates that $\sigma_{\rm sc}(H)$ is not monotonic: with increasing field $\sigma_{\rm sc}$ goes through the broad maximum at around 20 mT. The black solid line in Fig. 1(a), calculated within the model of Brandt [20], corresponds to $\sigma_{\rm sc}(H)$ for an isotropic s-wave superconductor with $\lambda = 360$ nm and $\kappa = \lambda / \xi \simeq 140$ ($\xi \simeq 2.6$ nm was obtained from the value of the second critical field $\mu_0 H_{c2}(0) \simeq 50$ T [21]). From

Fig. 1(a) we conclude that the experimental $\sigma_{sc}(H)$ depends much stronger on the magnetic field than expected for a fully gaped s-wave superconductor. As shown by Amin *et al.* [22] for a superconductor with nodes in the energy gap a field dependent correction to ρ_s arises from its nonlocal and nonlinear response to an applied magnetic field. The solid red line represents the result of the fit by means of the relation:

$$\frac{\rho_s(H)}{\rho_s(H=0)} = \frac{\sigma_{sc}(H)}{\sigma_{sc}(H=0)} = 1 - K\sqrt{H}, \qquad (4)$$

which takes the nonlinear correction to ρ_s for a superconductor with a d-wave energy gap into account [23]. Here the parameter K depends on the strength of the nonlinear effect. Since Eq. (4) is valid for intermediate fields $H_{c1} \ll H \ll H_{c2}$ (H_{c1} is the first critical field) only the data points above 40 mT were considered in the analysis.

We now discuss the T dependence of σ_{sc}. Figure 2 displays $\sigma_{sc}(T)$ measured at $\mu_0 H = 40$ mT. Below 20 K, σ_{sc} is linear in T as expected for a superconductor with nodes in the gap, consistent with the conclusion drawn from the analysis of the $\sigma_{sc}(H)$ data (see discussion above and Fig. 1). To ensure that $\sigma_{sc}(T)$ is determined primarily by the variance of the magnetic field within the VL we plot in Fig. 2(b) the corresponding $\alpha_s(T)$. It is constant from 1.6 K to $\simeq$27 K and drops to zero at $T \simeq 30$ K, where $P(B)$ becomes fully symmetric. A similarly sharp change of α_s with temperature was observed in Bi2212 and was explained by VL melting [14,15]. Correspondingly, we conclude that for temperatures $0 < T \lesssim 30$ K the T variation of σ_{sc} reflects the *intrinsic* behavior of the in-plane magnetic penetration depth λ_{ab}.

The T dependence of σ_{sc} was analyzed by assuming that the angular dependence of the energy gap in OP Bi2201 is similar to the one from recent ARPES experiments [3] [see Fig. 3(a)]. In analogy with Refs. [3,4] it was also assumed that the energy gap in the nodal region changes with temperature in accordance with the weak-coupling BCS prediction $\tilde{\Delta}(T/T_c) = \tanh\{1.82[1.018(T_c/T - 1)^{0.51}]\}$ [24], while the one near the antinodes is T independent [see the corresponding lines "A" and "B" in Fig. 3(b)]. The following cases were considered: (I) a monotonic d-wave gap $\Delta(T, \varphi) = 15$ meV $\cos(2\varphi)\tilde{\Delta}(T/T_c)$ (green dashed line); (II) a monotonic d-wave gap with suppressed quasiparticle weight in the antinodal region (solid orange line); (III) an analytical function, which follows the monotonic d wave 15 meV $\cos(2\varphi)\tilde{\Delta}(T/T_c)$ in the nodal region and changes to a 36 meV $\cos(3.4\varphi)$ behavior close to the antinodes (solid blue line). The T dependence of λ_{ab}^{-2} was calculated within the local (London) approximation ($\lambda \gg \xi$) using the following equation [13]:

$$\frac{\sigma_{sc}(T)}{\sigma_{sc}(0)} = 1 + \frac{8}{\pi - 4\varphi_0}\int_{\varphi_0}^{\pi/4}\int_{\Delta(T,\varphi)}^{\infty}\left(\frac{\partial f}{\partial E}\right) \times \frac{E dE d\varphi}{\sqrt{E^2 - \Delta(T,\varphi)^2}}. \qquad (5)$$

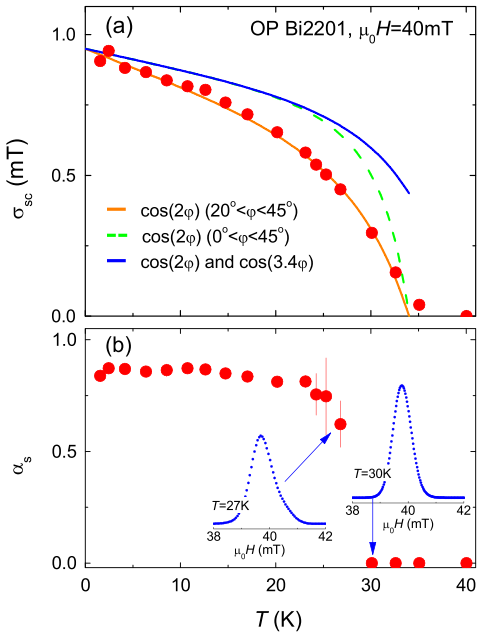

FIG. 2 (color online). (a) Dependence of σ_{sc} of OP Bi2201 on T measured at $\mu_0 H = 40$ mT. Lines represent the theoretical $\sigma_{sc}(T)$ curves obtained by assuming different symmetries of the superconducting energy gap [see Fig. 3(a)]. The errors in σ_{sc} are smaller than the size of data points. (b) Dependence of the skewness parameter α_s on T. The blue dotted curves represent $P(B)$ distributions below ($T = 27$ K) and above ($T = 30$ K) the VL melting temperature.

$f = [1 + \exp(E/k_B T)]^{-1}$ denotes the Fermi function. Here we also replace the prefactor $8/\pi$ of the integral with $8/(\pi - 4\varphi_0)$ to account for the case when the superconducting energy gap is developed only on a part of the

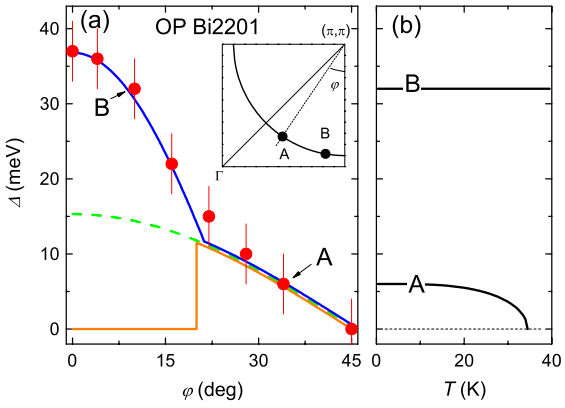

FIG. 3 (color online). (a) Angular dependence of the energy gap of OP Bi2201 obtained in ARPES experiments [3]. Lines represent the various models of the gap symmetries used to analyze the experimental $\sigma_{sc}(T)$ data [see Fig. 2(a)]. The inset shows schematically a part of the Fermi surface. The points "A" and "B" are close to the nodal ($\varphi \sim 45°$) and the antinodal ($\varphi \sim 0°$) region, respectively. (b) Temperature dependence of the energy gap in the nodal (curve A) and the antinodal (curve B) regions.

TABLE I. Transition temperature T_c, zero-temperature in-plane magnetic penetration depth $\lambda_{ab}^{-2}(0)$, and angular region where the superconducting d-wave gap is observed for OP Bi2201 (Ref. [3]), OP Na-CCOC (Refs. [6,7]), and OP La241 (Refs. [8,9]).

Compound	T_c (K)	$\lambda_{ab}^{-2}(0)$ (μm^{-2})	SC gap region
OP Bi2201	35	7.8(3)	$20° \lesssim \varphi < 45°$
OP Na-CCOC	28	10.0	$20° \lesssim \varphi < 45°$
OP La214	36	15.0	$0° \leq \varphi < 45°$

Fermi surface (in our case from φ_0 to $\pi/4$). The results of this analysis are presented in Fig. 2(a). The monotonic d-wave gap as well as the combined gap represented by the solid blue line in Fig. 3(a) cannot describe the experimental $\sigma_{sc}(T)$. Full consistency between ARPES and μSR data is obtained if one assumes a superconducting d-wave gap with only carriers in the region $20° \lesssim \varphi < 45°$ contributing to the superfluid [see Fig. 3(a)]. It should be noted here that the theoretical $\sigma_{sc}(T)$ curves in Fig. 2 were not fitted, but obtained directly by introducing the angular dependence of the gap measured in ARPES experiments into Eq. (5), describing the T dependence of the penetration depth within the London approach.

Next we compare the zero-temperature values of $\lambda_{ab}^{-2}(0) \propto n_s/m^*$ for various OP HTS's having comparable T_c values and for which the angular dependence of the superconducting gap was measured [3,6,9]. OP La214, which exhibits a fully developed superconducting gap, has an approximately 50% higher value of the superfluid density as compared to both OP Na-CCOC and OP Bi2201, having the superconducting gap opened only on a limited part of the Fermi surface (see Table I). Assuming that the supercarrier masses m^* are the same for all OP compounds listed in Table I (in analogy with $m^* \simeq 3 - 4m_e$ reported for La214 and $YBa_2Cu_3O_{7-\delta}$ families of HTS's [25]), the difference in the values of $\lambda_{ab}^{-2}(0)$ can be naturally explained by the different number of carriers condensed into the superfluid. In the case of OP Bi2201 and OP Na-CCOC, n_s is strongly reduced because of the fraction of the states is no more available for the superconducting condensate due to the pseudogap.

To conclude, the in-plane magnetic penetration depth λ_{ab} in optimally doped Bi2201 was studied by means of muon-spin rotation. By comparing the measured $\lambda_{ab}^{-2}(T)$ with the one calculated theoretically using a model consistent with ARPES measurement [3] we found that the superconducting gap in OP Bi2201 has d-wave symmetry, but only carriers from parts of the Fermi surface close to the node ($20° \lesssim \varphi \lesssim 45°$) contribute to the superfluid. This implies that the pseudogap affects the spectral density of the quasiparticles and, consequently, not all the states at the Fermi surface are available to participate in the superconducting condensate. Our results supports the scenario where the superconducting and pseudogap state are two distinct and competing phenomena. This statement is also consistent with the fact that the superfluid density in OP Bi2201 is strongly reduced in comparison with that in OP La214, where the superconducting gap and coherent quasiparticles are observed along the whole Fermi surface ($0° \leq \varphi < 45°$) [9].

This work was performed at the Swiss Muon Source (SμS), Paul Scherrer Institute (PSI, Switzerland). The authors are grateful to Y. J. Uemura and R. Prozorov for stimulating discussions, and S. Weyeneth for performing torque experiments. This work was supported by the K. Alex Müller Foundation and in part by the Swiss National Science Foundation. Work at the Ames Laboratory was supported by the Department of Energy-Basic Energy Sciences under Contract No. DE-AC02-07CH11358.

*rustem.khasanov@psi.ch

[1] M. Le Tacon *et al.*, Nature Phys. **2**, 537 (2006).
[2] K. Tanaka *et al.*, Science **314**, 1910 (2006).
[3] T. Kondo *et al.*, Phys. Rev. Lett. **98**, 267004 (2007).
[4] W. S. Lee *et al.*, Nature (London) **450**, 81 (2007).
[5] W. Guyard *et al.*, Phys. Rev. B **77**, 024524 (2008).
[6] T. Hanaguri *et al.*, Nature Phys. **3**, 865 (2007).
[7] R. Khasanov *et al.*, Phys. Rev. B **76**, 094505 (2007).
[8] C. Panagopoulos *et al.*, Phys. Rev. B **60**, 14617 (1999).
[9] M. Shi *et al.*, Phys. Rev. Lett. **101**, 047002 (2008).
[10] T. Kondo *et al.*, J. Electron Spectrosc. Relat. Phenom. **137–140**, 663 (2004); T. Kondo *et al.*, Phys. Rev. B **72**, 024533 (2005).
[11] J. E. Sonier, J. H. Brewer, and R. F. Kiefl, Rev. Mod. Phys. **72**, 769 (2000).
[12] R. Khasanov *et al.*, Phys. Rev. B **73**, 214528 (2006).
[13] R. Khasanov *et al.*, Phys. Rev. Lett. **98**, 057007 (2007).
[14] S. L. Lee *et al.*, Phys. Rev. Lett. **71**, 3862 (1993).
[15] C. M. Aegerter *et al.*, Phys. Rev. B **57**, 1253 (1998).
[16] T. M. Riseman *et al.*, Phys. Rev. B **52**, 10569 (1995).
[17] P. L. Russo *et al.*, Phys. Rev. B **75**, 054511 (2007).
[18] S. Weyeneth (to be published).
[19] S. Kawamata *et al.*, J. Low Temp. Phys. **117**, 891 (1999).
[20] E. H. Brandt, Phys. Rev. B **68**, 054506 (2003).
[21] Y. Wang *et al.*, Science **299**, 86 (2003).
[22] M. H. S. Amin, M. Franz, and I. Affleck, Phys. Rev. Lett. **84**, 5864 (2000).
[23] I. Vekhter, J. P. Carbotte, and E. J. Nicol, Phys. Rev. B **59**, 1417 (1999).
[24] A. Carrington and F. Manzano, Physica (Amsterdam) **385C**, 205 (2003).
[25] W. J. Padilla *et al.*, Phys. Rev. B **72**, 060511 (2005).